JOURNAL OF MATERIALS SCIENCE **33** (1998) 5509–5516

Mechanical properties of aluminium/Inconel 601 composite wires formed by swaging

C. SALMON, F. BOLAND, C. COLIN*, F. DELANNAY
Université catholique de Louvain, Département de sciences des matériaux et des procédés, PCIM, Place Sainte Barbe 2, B-1348 Louvain-la-Neuve, Belgium

This work investigates the formability of a composite made of a pure aluminium matrix reinforced with an Inconel fibre network. Composites were formed into wires by swaging, to a true strain $\varepsilon_{true} = 2.7$. Thermal expansion, Young's modulus and tensile properties of these wires were measured. Young's modulus of the wires is slightly larger than that of the as-cast composites, indicating that no significant porosity is present in the composite after deformation. Tensile strength and ductility are found to decrease with increasing reduction of diameter. Scanning electron microscope (SEM) observations show that fibres align during swaging and that fibre fragmentation occurs beyond a certain strain. Fibre fragments reach a critical aspect ratio of about 7 after a swaging true strain of 1.5. Qualitatively, the evolution of the properties is explained by a combination of fibre fragmentation and fibre alignment effects. Properties of the wires are discussed using the Clyne model and the Nardone and Prewo model (modified shear lag models).

1. Introduction

A large variety of ceramic fibres have been used for reinforcing Al alloys. Beside an attractive high-temperature strength, Al/ceramic fibres composites usually present low ductility and low toughness. On that point of view, the use of ductile metallic fibres for reinforcing Al alloys appears as an interesting possible alternative because metallic fibres can improve the strength without causing a too large loss of ductility. Little work has been done on composites made of an Al alloy reinforced with metallic fibres because the high reactivity of Al with most metals brings about the formation of brittle intermetallic compounds which cause a catastrophic loss of toughness. Nevertheless, it has recently been reported that the control of processing conditions makes possible the production of sound Al-based composites reinforced with metallic fibres [1]. These processing conditions involve a high solidification rate and the reduction of the reactivity between the fibres and the matrix either by use of alloying additions in the matrix or by surface treatment of the fibres. It was demonstrated that Al-matrix composites reinforced with heat-treatment nickel-base alloy fibres (Inconel 601 – diameter 12 μm) could be produced by squeeze-casting. Thanks to the oxidic barrier formed on the fibres during heat-treated, neither interface reaction layer nor dissolution of the elements of the fibres was observed in these composites. Tensile tests showed that the addition of 20% of fibres in pure aluminium induces a strength increase by more than a factor of 2.5 at room temperature [1]. Moreover, whereas metallic composites usually reach only a few per cent ductility, these composites present a ductility of about 8%. High temperature tensile properties are also significantly improved. Hence, the use of such metallic fibre reinforced composites could be interesting for applications where high-temperature strength is needed but where the density of the material does not matter too much.

This paper aims at exploring the formability of aluminium/Inconel fibres composites. Only pure aluminium was considered for the matrix. Indeed, pure Al reinforced with metallic fibres constitutes a model system that allows investigation of the plastic behaviour of two interconnected ductile phases deforming together. Testing of the formability of such a system of interconnected phases is of great interest. The possibility of making wires of plates by plastic forming broadens the possible range of uses of metallic fibre reinforced composites. Particularly, a good formability into wires allows the fabrication of composite electrical wires whose thermal expansion coefficient is reduced.

In this study, an investigation of the mechanical and thermal properties of composite wires produced by swaging (rotative hammering) is presented. From the evolution of these properties as a function of swaging true strain, an analysis is made of how the two phases behave when strained together. The modified shear lag model introduced by Clyne [2] for composites with a relatively small modulus mismatch is used to predict the Young's modulus of the wires and the tensile strength

* Ecole nationale supérieure des mines de Paris, Centre des matériaux P-M Fourt, BP 87, F-91003 Evry Cedex, France.

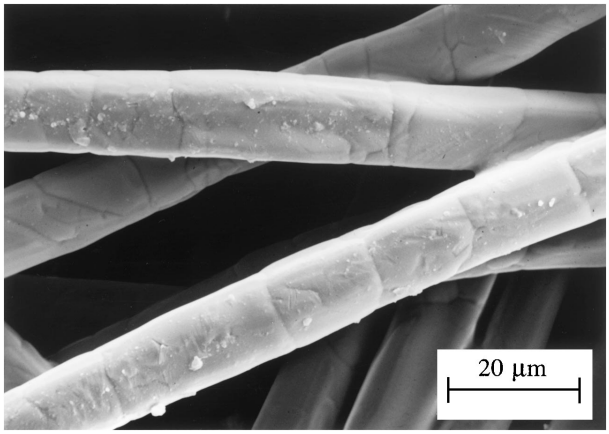

Figure 1 SEM micrograph of the Inconel 601 fibres.

of the fibres while the Nardone and Prewo model [3] is used to predict the yield strength of the wires.

2. Experimental

Use was made of 10 mm thick performs consisting of 22 ± 1 vol % of 12 μm diameter continuous Inconel 601 fibres (N.V.Bekaert S.A.) [4]. The preforms are made by stacking loose felts of planar randomly oriented fibres and by sintering the stack in order to form strong interconnections at fibres crossings. The performs thus present transverse isotropy. During sintering, fibres grains grow to a size about equal to the fibre diameter, as presented in Fig. 1. Thanks to the ductility of the fibres, their volume fraction in the composite can be easily varied from 20 to 80% by compacting the sintered preforms before infiltration with the matrix alloy. Only volume fraction of 20% was considered in this study.

To prevent the reaction from appearing when Al comes into contact with Inconel during processing of the composites, the fibres preforms were heat-treated in air at 750 °C during 30 min. This leads to the formation of an oxidic passivation layer at the surface of the fibres. This oxidation condition was found to be optimal as far as the mechanical properties of the composites are concerned. After heat-treatment, the preforms were infiltrated with pure liquid aluminium using the squeeze casting method already described in previous papers [5, 6].

In order to swage these composites into wires, rods with diameters varying from 6 to 9 mm were machined in the cast. The composites were swaged in several steps using dies with decreasing diameters (about 10% diameter reduction at each step). Each reduction of diameter was followed by annealing at 375 °C for 15 min. These conditions of the annealing treatment were optimised (using hardness and microhardness tests) in order to restore ductility without inducing interface reaction. Composites wires were produced by swaging down to a diameter reduction of 74%, which corresponds to a true strain of 2.7 (wire diameter of about 2 mm).

Young's modulus and tensile properties were measured on as-cast composites and on formed composite wires. Only the in-plane properties of the as-cast composites were tested. Young's modulus was evaluated on

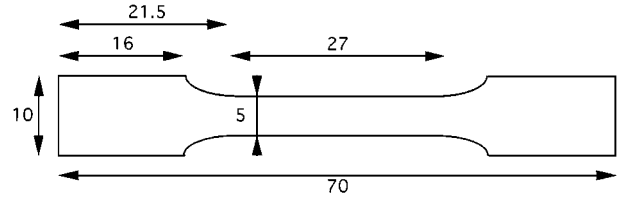

Figure 2 Size of the tensile specimens machined in the as-cast composites.

cuboid bars (as-cast materials) and cylinders of different diameters (swaged materials) using the resonance frequency method (grindosonic) in bending, assuming isotropic properties with a Poisson ratio $\nu = 0.3$. Tensile properties of the as-cast composites and of the wires were evaluated by tensile tests at room temperature at a rate of 0.2 mm/min. The elongation was measured using an extensometer with 25 mm gauge length. Samples of 60 to 80 mm length were cut from the wires swaged to different diameters. In order to prevent local deformation of the heads of the wire specimen in the grips, the heads were embedded into two half hollow cylinders made of Al alloy. The dimensions of the as-cast tensile specimens machined in the as-cast composites are given in Fig. 2.

For the study of the thermal expansion behaviour, three cycles between room temperature and 300 °C were carried at 1 °C/min out in air on cuboid bar or cylinder specimens with 10 to 30 mm length. A dwell was carried out at 300 °C during the two first cycles in order to relax the internal stresses. The linear thermal expansion coefficient of the composites was measured during the cooling stage of the third cycle. The CTE of pure Al (99.99 wt %) was measured between 25 °C and 300 °C to test the calibration of the dilatometer. The measured average value of $24.5 \pm 0.7 \times 10^{-6}$ K^{-1} is in good agreement with the value of 25.3×10^{-6} K^{-1} reported in the literature [7]. The thermal expansion coefficient of Inconel 601 is 17.1×10^{-6} K^{-1} [8].

3. Results

3.1. As-cast composites

Fig. 3 illustrates the typical microstructure of a squeeze-cast composite containing 20 vol % of Inconel 601 fibres, before forming. At the resolution of the SEM imaging, the composite appears to be devoid of any porosity, even at concave solid angles at fibres contacts. The absence of significant porosity was confirmed by density measurements performed by the Archimedean method. The thin black layer at the fibre/matrix interface may reflect the presence of the passivation layer on the fibres. TEM analyses confirmed the absence of any reaction layer at fibre/matrix interface and indicated that the mean thickness of the oxides layer was about 300 nm.

Fig. 4 shows the typical evolution of strain during the third cycle of the thermal expansion test performed on pure Al and on as-cast Al/In601 composites, in the direction of the fibres plane (in-plane) and in the direction perpendicular to this plane (transverse). The composite presents a sharply reduced average expansivity between

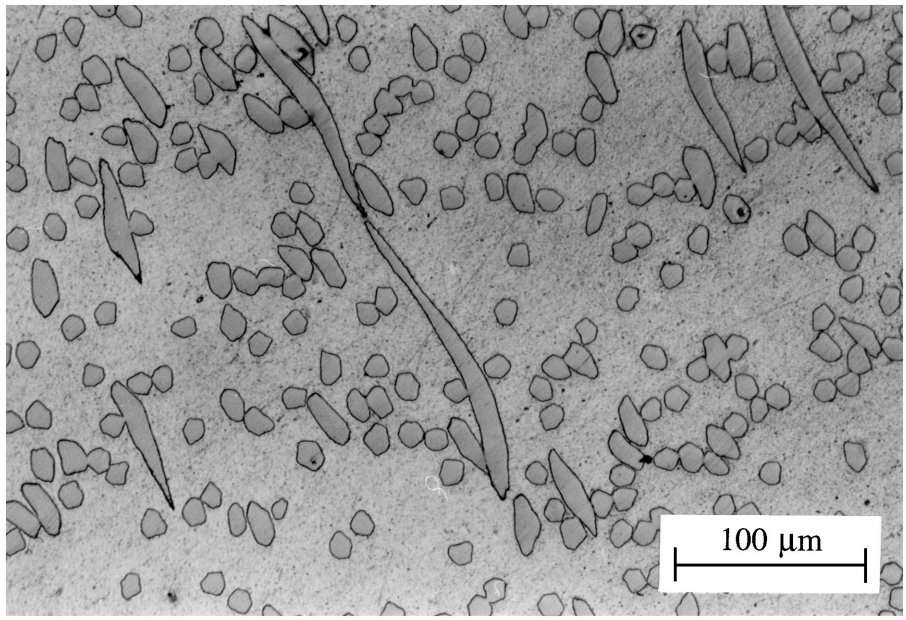

Figure 3 Optical micrograph of an as-cast Al-20% In601 composite processed using a preform heat-treated at 750 °C during 30 min in air.

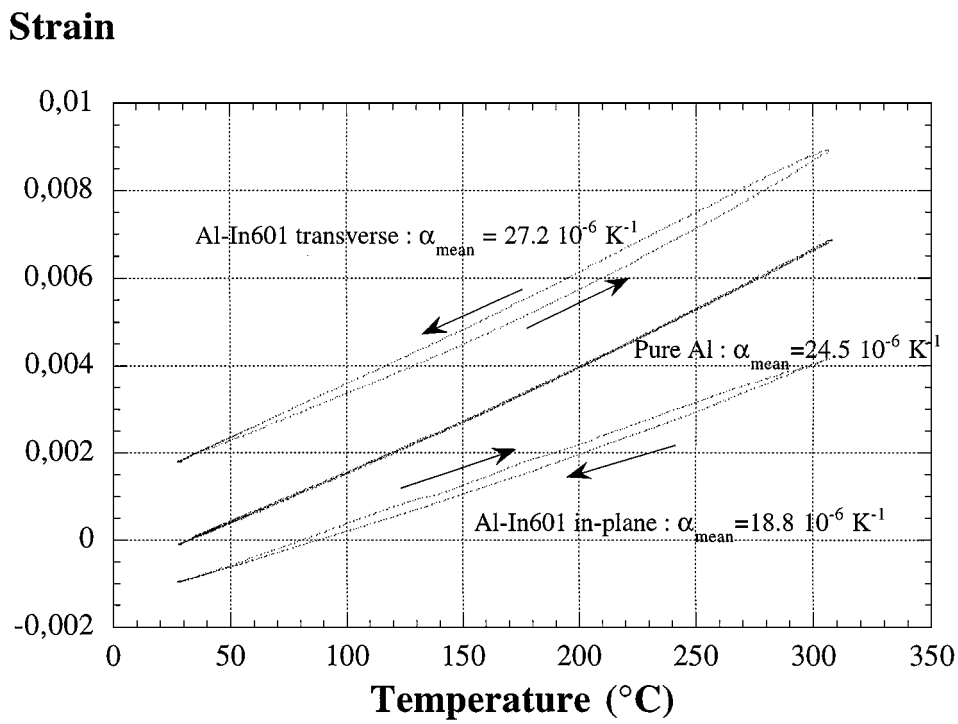

Figure 4 Third cycle of a thermal expansion test, for pure Al and for an Al-20% In601 composite tested in the plane of the fibres and in the direction perpendicular to this plane.

room temperature and 300 °C in the in-plane direction ($\alpha = 18.8 \pm 1.3 \times 10^{-6}\,\mathrm{K}^{-1}$), which is compensated by an increase of the expansivity in the transverse direction ($\alpha = 27.2 \pm 1.3 \times 10^{-6}\,\mathrm{K}^{-1}$) (this difference is not unexpected as volume is conserved during thermal cycling). The hysteresis loop observed for the composite indicates that thermal mismatch stresses cause plastic yielding in the matrix.

3.2. Composite wires

After the shaping of the composites by swaging, the microstructure of transverse sections of the wires was studied by optical microscopy and by SEM. No damage in the matrix or at the fibre/matrix interface could be detected.

The average thermal expansion coefficients of the swaged and as-cast composites between 25 and 300 °C are compared in Fig. 5. Thermal expansion decreases slightly from $\alpha = 18.8 \pm 1.3 \times 10^{-6}\,\mathrm{K}^{-1}$ in the as-cast condition to $\alpha = 16.4 \pm 0.6 \times 10^{-6}\,\mathrm{K}^{-1}$ at a true strain $\varepsilon_{\mathrm{true}} = 0.6$. It does not seem to evolve anymore for larger strain.

Fig. 6 compares the Young's modulus of swaged and as-cast composites. The fibre volume fraction of each specimen was measured by density measurements. The

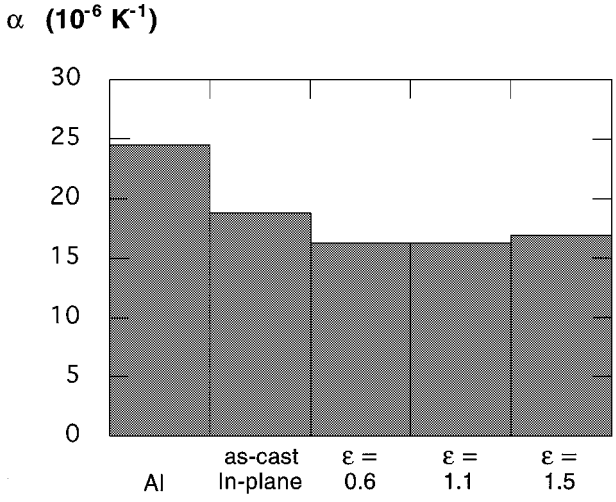

Figure 5 Average thermal expansion coefficient between 25 °C and 300 °C for as-cast Al/In601 composite (in-plane) and for composites swaged up to different true strains.

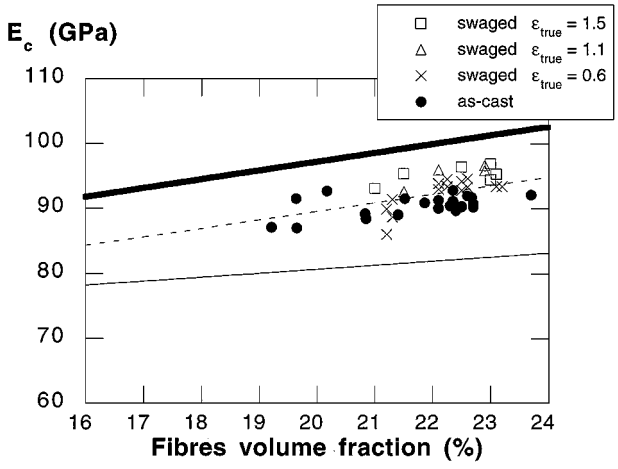

Figure 6 Young's modulus of as-cast and swaged composites (▬ Voigt bound, ▬ Reuss bound and ------ modified shear lag model [7]).

scattering is due to the small size of the specimens. All results locate between the Voigt and Reuss bounds computed using $E_{Al} = 70$ GPa and $E_{In601} = 206$ GPa [8]. This further attests for the absence of porosity in the composites. Young's modulus of swaged samples is, on the average, higher than that of the as-cast samples, suggesting no damage in the composite during forming.

Fig. 7 presents the engineering stress-strain curves of swaged composites after different swaging extents. Strength is observed to decrease progressively with increasing diameter reduction. The tensile ductility varies between 1 and 7%, indicating a large scattering. These values are lower than the ductility of $8 \pm 2\%$ measured for the as-cast composites [1]. The evolutions of the yield strength ($\sigma_{0.2\%}$) and of the tensile strength (σ_{TS}) with swaging strain are summarized on Fig. 8. For a swaging true strain $\varepsilon_{true} = 0.35$ (diameter reduction = 16%), $\sigma_{0.2\%}$ increases by 40% and σ_{TS} by 30% in comparison to the as-cast composite. Subsequently, both $\sigma_{0.2\%}$ and σ_{TS} decrease with increasing swaging strain, reaching values similar to that of the as-cast composite for $\varepsilon_{true} \cong 1.5$ (diameter reduction = 53%).

Damage development during tensile testing was evaluated by measuring the decrease of the density and Young's modulus after tensile fracture. For this purpose, sections were cut within the uniform deformation zone in specimens which had exhibited approximately the same uniform strain $\varepsilon_t \cong 0.04$ before fracture. Density measurements by the Archimedean method and modulus measurements by the grindo-sonic method were compared to the values obtained before tensile tests. Although the dispersion was high, we observed a trend to a decrease of modulus and of density with increasing swaging strain. However the variations were slight: for a swaging true strain of 1.5, the decrease of density amounted to a few tenth of a percent and the decrease of modulus to about 6%.

In order to evaluate the influence of the forming process on the strain-hardening of both phases, microhardness tests were performed on as-cast composites and on samples swaged to a true strain $\varepsilon_t \cong 2$ before and after annealing at 375 °C for 15 min. Fig. 9a shows that the matrix strain-hardens quite a bit during forming and that the annealing treatment is sufficient to restore its ductility. Strain-hardening of the fibres is illustrated in Fig. 9b. Considering the standard deviation of the results, the strain-hardening of the fibres appears quite limited. As expected, this strain-hardening of the fibres is not affected by annealing at 375 °C.

The SEM micrograph on Fig. 10 presents the morphology of the fibre network after a diameter reduction of 74% (swaging true strain = 2.7). The fibres close to the surface have been separated from the matrix by deeply etching the composite surface after polishing. It is observed that, during forming, fibres have oriented along the axis of the wire and have broken. From a randomly oriented continuous fibre composite, swaging has produced an aligned short fibre composite. Fibres break after a critical value of diameter reduction: SEM analyses of composites with different extents of swaging indicated that this critical value corresponds to a true strain of about 0.35 (see Table I).

Fig. 11a presents the evolution of the average length of the fibre fragments as a function of the true strain.

TABLE I Evolution of the preform aspect, of the mean length of broken fibres and of the fibres diameter as a function of the true strain undergone by the composite during swaging

True strain	Preform aspect	Mean length of the broken fibres (μm)	Fibre diameter (μm)
0	Network	—	12.5 ± 0.8
0.35	Some fibres breaking	—	
0.60	Some fibres breaking	—	11.7 ± 0.9
1.10	Central network + short fibres	103 ± 36	12.4 ± 0.9
1.50	No more network, short fibres	84 ± 31	11.5 ± 1.1
2.00	No more network, short fibres	75 ± 28	12.8 ± 1.0
2.70	No more network, short fibres	82 ± 36	11.0 ± 1.5

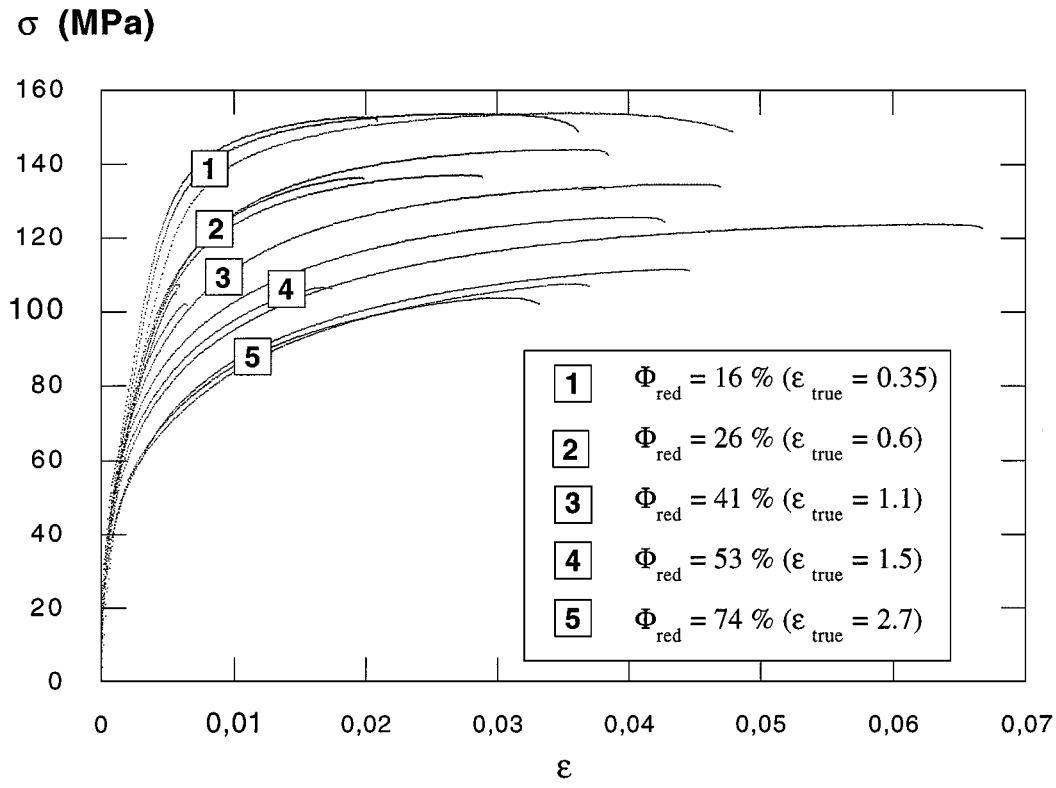

Figure 7 Conventional stress-strain curves of composites swaged to different diameter reductions.

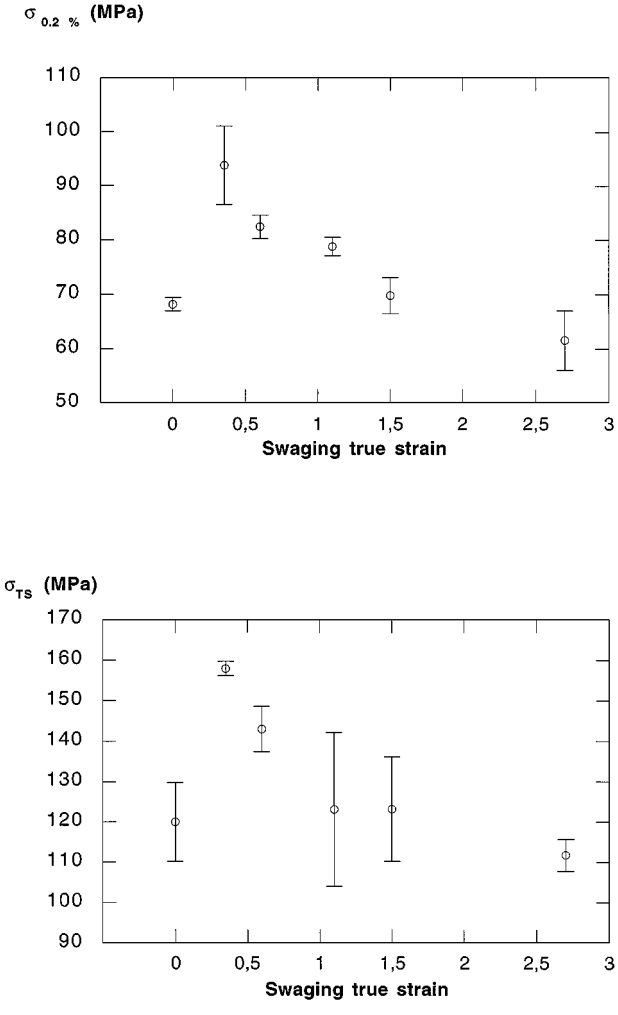

Figure 8 Evolution of (a) conventional yield strength $\sigma_{0.2\%}$ and (b) ultimate tensile strength σ_{TS} of the composites as a function of the swaging true strain.

The average fibre length was measured by dissolving the Al matrix in HCI and by measuring the length of about 300 fibres on SEM images such as Fig. 10. A typical length distribution is shown on Fig. 11b. More detail about the morphology of the fibre preforms after forming is given in Table I. SEM observation of the fibres after complete leaching out the matrix showed that the fragmentation of the fibres was not uniform in the wire section. For a strain $\varepsilon_t \leq 1.5$, fibres are broken only at the wire periphery and an interconnected fibre network still remains in the centre of the wire. For $\varepsilon_t \geq 1.5$, only short fibre fragments are found. Fibres seem to have reached a minimum length of about 80 μm after a true strain of 1.5. As indicated in Table I, the fibre diameter does not seem to change in spite of the progressive diameter reduction of the composite.

It is worth mentioning that rolling tests performed on the same composites showed the same behaviour: fibre breaking begins for quite the same equivalent true strain and an average minimum fibre length of about 80 μm is also measured.

4. Discussion

From the observation of the microstructure of the composites and of the morphology of the preforms at different stages of the forming process, we can conclude that:

1. During the first steps of the process, the fibres align in the direction of the axis of the wire, without being deformed ($\varepsilon_t = 0$ to 0.3).
2. After a critical amount of swaging, when aligning is completed, fibres begin to break. The fibres at the surface of the wires appear to break first ($\varepsilon_t = 0.3$ to 1.1).

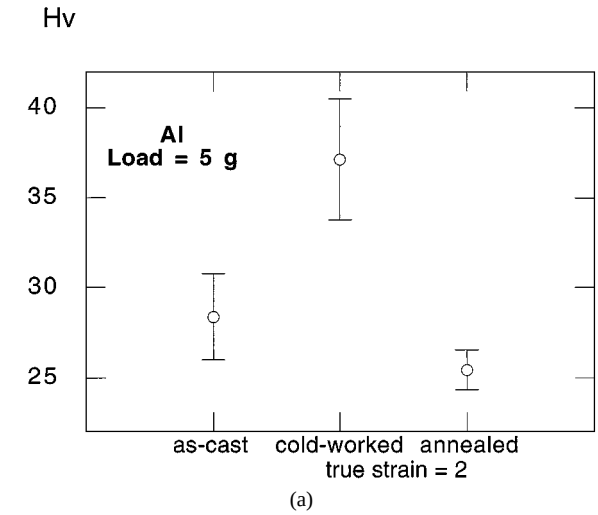

(a)

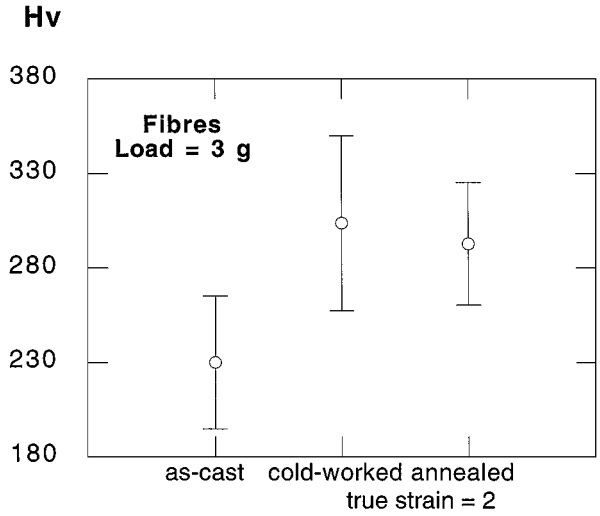

(b)

Figure 9 Vickers microhardness of (a) the aluminium matrix (load = 5 g) and (b) the Inconel fibres (load = 3 g) in the as-cast composite and in composites swaged to a true strain of 2, before and after annealing at 375 °C for 15 min.

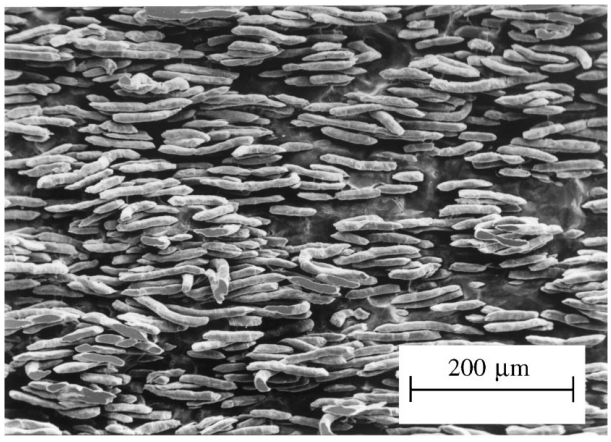

Figure 10 SEM micrograph of a swaged composite after a diameter reduction of 74%. The sample was deeply etched in HCl.

3. Finally, fibres breaking propagates to the centre of the wire until the fragments assume a mean aspect ratio of about 7 ($\varepsilon_t = 1.1$ to 2.7). No significant change of the fibre diameter is observed.

Several features can have an influence on the value of the Young's modulus of the composite:

- the orientation of the fibres,
- the aspect ratio of the fibres,
- the porosity (or damage) in the composite.

No porosity could be detected at the SEM resolution. In addition, the modulus of swaged composites is globally higher than that of the as-cast composites (Fig. 6). This suggests that the modulus increase due to the fibre alignment outbalances the modulus decrease due to the decrease of the aspect ratio.

A convenient model for estimating the Young's modulus of an aligned short fibres composites with an aspect ratio of 7 is the "modified shear lag model" proposed by Clyne [2]. According to this model:

$$E_c = \left\{ V_f E_f \left[1 - \frac{(E_f - E_m^*)\tanh(ns)}{E_f ns} \right] + V_m E_m \right\} \quad (1)$$

where

$$E_m^* = \frac{E_f(1 - \mathrm{sech}(ns)) + E_m}{2} \quad (2)$$

and

$$n = \left\{ \frac{2E_m}{E_f(1+\nu_m)\ln(1/V_f)} \right\}^{1/2} \quad (3)$$

E_c, E_f and E_m are the Young's modulus of the composite, fibres and matrix, respectively, ν_m is the Poisson ratio of the matrix, V_f and V_m are the fibre and matrix volume fraction, and s is the mean fibre aspect ratio. The result presented as a dotted line on Fig. 5 is obtained using $s = 7$, $E_m = 70$ GPa, $E_f = 206$ GPa and $\nu_m = 0.3$. Although porosity is not taken into account, the prediction of the model underestimates the measured values. Considering the experimental scatter, it does not seem worth further commenting the difference between the model and the results. We at least can conclude that no significant porosity is present in the composites.

The slight decrease of the average thermal expansion coefficient of the composite after swaging (Fig. 5) can also be explained by the prevalence of fibre alignment on fibre fragmentation. Thermal expansion cannot be simulated by a linear thermoelasticity model because, as shown on Fig. 4, some plastic yielding has occurred in the matrix during the test.

The major parameters determining the yield strength and tensile strength of composites are:

- the orientation of the fibres,
- the aspect ratio of the fibres,
- the strain hardening of the fibres,
- the strain hardening of the matrix,
- the damaging of the material.

Fig. 8a shows that $\sigma_{0.2\%}$ first increases during the forming process and decreases subsequently with increasing true strain, reaching finally values lower than for the

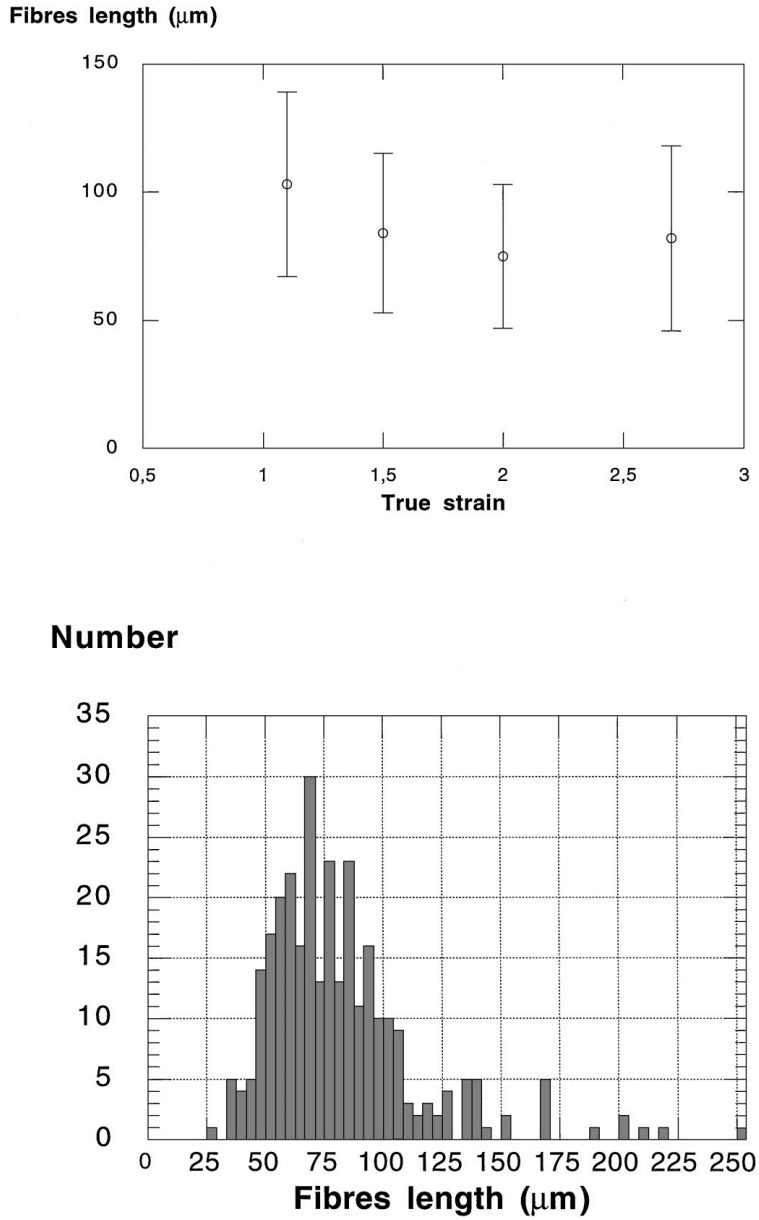

Figure 11 (a) Mean length of the fibre fragments as a function of the true strain in swaging. (b) Typical fibre length distribution (sample swaged to a true strain $\varepsilon_t = 2.7$).

as-cast composite. This evolution of the properties could be qualitatively explained as follows:

1. At the beginning of swaging, strain-hardening of the fibres and alignment of the fibres give rise to an increasing strength.
2. The strength increase due to fibre alignment is rapidly outbalanced by the decrease of the aspect ratio, in such a way that, globally, the strength decreases progressively with increasing strain.

We can try to predict the yield strength of the swaged composite using the equation derived by Nardone and Prewo [3] also on the basis of the shear lag model. These authors express the yield strength as

$$\sigma_{cy} = \sigma_{my}\left[V_f\frac{(s+2)}{2} + V_m\right] \qquad (4)$$

where σ_{my} and σ_{cy} are the yield strength of the matrix and of the composite, respectively. Assuming aligned short fibres with an aspect ratio of 7 and using $\sigma_{my} = 25$ MPa [1], we find $\sigma_{cy} = 43$ MPa, to be compared to the measured value $\sigma_{0.2\%} = 70$ MPa. Sekine and Chen [9] explain the underestimation brought about by the shear lag model by the effect of matrix hardening. Indeed, the yield strength of the matrix is increased because of a higher dislocation density (due to thermal mismatch between matrix and fibres) and of a smaller grain size. For the present composites, the yield strength of the matrix should be increased from 25 to 40 MPa to yield a prediction in agreement with experiment. Such a strength increase is not unrealistic for a pure Al matrix.

The value of the tensile strength of the fibres after sintering and infiltration is not known. However, the minimum critical aspect ration of the fibres, after extensive swaging can be used to evaluate the tensile strength of the fibres, σ_f, by using again the relation derived from the shear lag model [10]:

$$s = \frac{l_c}{d_f} = \frac{\sigma_f}{2\tau_{my}} \qquad (5)$$

where l_c is the critical length of the fibres, d_f is the diameter of the fibres, and τ_{my} is the shear strength of the matrix. Using $\tau_{my} = \sigma_{my}/2 = 12.5$ MPa and $s = 7$, relation (5) gives $\sigma_f = 175$ MPa. Using $\sigma_{my} = 40$ MPa for accounting for the matrix strengthening, we find $\sigma_f = 280$ MPa. These values seem quite low for Inconel 601, even considering the effect of the annealing brought about by the sintering treatment. In his modified shear lag model, Clyne [2] proposes the relation

$$s = \frac{l_c}{d_f} = \frac{\sigma_f}{2\tau_{my}}\left(\frac{E_f - E_m}{2E_f}\right) \qquad (6)$$

In this case, using the same value of s, one obtains $\sigma_f = 530$ MPa with $\tau_{my} = 12.5$ MPa and $\sigma_f = 850$ MPa with $\tau_{my} = 20$ MPa. It thus appears that the modified shear lag model can predict our results rather satisfactorily. The advantage of the shear lag analysis is its simplicity in comparison to models requiring complex numerical procedures. Indeed, the 'modified' shear lag model was proven to give predictions of elastic properties of MMCs very close to the predictions of the Eshelby model.

The evolution of the tensile strength σ_{TS} of the composites as a function of the swaging true strain can be interpreted by invoking the same phenomena as for the evolution of the yield strength σ_{my}. Moreover, if significant, the slight further decrease of the strength at $\varepsilon_t \geq 1.5$, i.e. when the alignment is maximum and when the aspect ratio has reached a constant minimum value, may perhaps be explained by some damaging of the material. During tensile straining of the composite, voids can nucleate at the ends of fibre fragments. The slight decrease of density and Young's modulus after tensile testing might be due to the presence of such voids. Moreover, the reduced ductility of the swaged composites (Fig. 7) indicates that these composites are more sensitive to damage than as-cast composites.

5. Conclusions

This work demonstrates that the high ductility of aluminium matrix composites reinforced with Inconel fibres allows rather good formability. The Al/In601 composites can be formed to a true strain of 2.7 by swaging. No porosity nor defect can be detected in the composite wires. The different resistance of fibre and matrix to plastic straining brings about fibre fragmentaiton during forming. It has been shown that the fibre fragments rapidly reach a minimum aspect ratio of about 7. This value can be justified considering the flow strength of the matrix and of the fibres. The mechanical properties of the wires could be explained semi-quantitatively using the modified shear lag model considering the effects of both fragmentation and alignment of the fibres.

Acknowledgements

The Inconel 601 fibre preforms used in this work were supplied by N. V. Bekaert S.A. This work was carried out under financial support of Region Wallonne (Belgium, contract no. 2386), of the European Union (Copernicus program, CIPA-CT94-0192) and of SSTC (Belgium, PAI action P4/33).

References

1. F. BOLAND, Ph.D. Thesis Université catholique de Louvain, 1996.
2. T. W. CLYNE, *Mater. Sci. Eng.* **A122** (1989) 183–192.
3. V. C. NARDONE and K. M. PREWO, *Scripta Metallurgica* **20** (1986) 79–91.
4. R. DE. BRUYNE, *Advances in Powder Metallurgy and Particulate Materials* **5** (1996) 16–99.
5. L. TAO, M-A. DELLIS, F. BOLAND and F. DELANNAY, *Composites* **26** (1995) 611–617.
6. C. COLIN, Y. MARCHAL, F. BOLAND and F. DELANNAY, *J. de Physique IV*, Colloque C7, supplément au journal de physique III, **3** (1993) 1749.
7. A. BRANDES, "Smithells Metals Reference Book" (Butterworths, London, 1983) p. 14.
8. J. L. EVERHART, "Engineering Properties of Nickel and Nickel Alloys" (Plenum Press, New-York, London, 1971).
9. H. SEKINE and R. CHEN, *Composites* **26**(3) (1995) 183–188.
10. H. L. COX, *Br. J. Appl. Phys.* **3** (1952) 72–79.

Received 16 June
and accepted 15 September 1998